

Beta-decay asymmetry from the decays of oriented ^{52}Mn and $^{60}\text{Co}^\dagger$

S. T.-C. Hung,* K. S. Krane, \ddagger and D. A. Shirley

*Department of Chemistry and Lawrence Berkeley Laboratory
University of California, Berkeley, California 94720*

(Received 19 May 1975; revised manuscript received 24 November 1975)

The β decay of ^{52}Mn has been investigated by measuring the angular distribution asymmetry of the positrons emitted from ^{52}Mn oriented at low temperatures. The ^{52}Mn nuclei were polarized in an iron lattice and cooled by thermal contact with an adiabatically demagnetized paramagnetic salt. The positron asymmetry was determined by means of two independent techniques: The positrons were detected directly using high-purity germanium detectors and indirectly using NaI detectors to observe the annihilation γ rays. These two techniques yielded a consistent result for the asymmetry, corresponding for this allowed decay to a ratio of the Fermi to Gamow-Teller matrix elements of $y = C_V M_F / C_A M_{GT} = -0.144 \pm 0.006$. An auxiliary experiment on ^{60}Co gave a β asymmetry $A = -0.971 \pm 0.034$, in excellent agreement with the theoretical value of -1 expected for maximal parity violation.

RADIOACTIVITY ^{52}Mn , ^{60}Co ; measured β asymmetry, deduced Fermi/
Gamow-Teller ratio in ^{52}Mn decay.

I. INTRODUCTION

The study of the angular distribution of radiation emitted by oriented nuclei has proven to be a powerful and convenient means of deducing the properties of nuclear radiation fields, in particular their multipole character. In the case of allowed β decay, such studies can be analyzed to yield the ratio of the Fermi (F) to Gamow-Teller (GT) matrix elements in the β decay, from which ratio one can deduce in turn the degree of isospin mixing in the nuclear states (isospin selection rules forbid the emission of Fermi-type decays between low-lying states of pure isospin) and the magnitude of the charge-dependent nuclear matrix elements. Comprehensive reviews of the theoretical background necessary for interpretation of the results of this type of experiment, as well as summaries of experimental results, may be found in the works of Schopper¹ and of Wu and Moskowski.² The present report contains a description of a measurement of the angular distribution asymmetry in the allowed positron β decay of oriented ^{52}Mn .

A compelling justification for undertaking a more precise determination of the F/GT ratio is based on the search for evidence of violations of fundamental symmetries in nuclei. In particular, in recent years numerous experimental studies have been made to search for evidence of parity (P) and time-reversal (T) violation in nuclei. Although no direct evidence for T violation has yet been obtained, indirect evidence results from the observation of CP violation in the K_0 decay,³ and there is speculation as to whether this effect arises from

T violation in weak or electromagnetic interactions. In the case of allowed β decay, T violation would be manifest as a complex phase of the F/GT ratio; furthermore, as the size of the T -violating observable is proportional to $y/(1+y^2)$, where y is the ratio of Fermi to Gamow-Teller amplitudes, it is advisable to choose a case for investigation in which there is reasonable interference between the F and GT terms. Previous determinations of the ratio y in ^{52}Mn have not been in good agreement, and the possibility that a large value of y might make ^{52}Mn a favorable candidate for an investigation of T violation in β decay has in part prompted the present remeasurement.

The F/GT ratio y may be determined from a measurement of the angular distribution anisotropy of β particles relative to an axis of nuclear polarization. This may be implemented either (1) by observing the anisotropy of β emission relative to the nuclear polarization axis (using an external polarizing field applied to nuclei cooled to ultralow temperatures⁴), or (2) by observing the angular correlation between the direction of β emission (from an unpolarized nuclear state) and the direction of a subsequent coincident γ ray, whose circular polarization must be detected.⁵ Each of these two techniques suffers from serious difficulties, mostly involving the extraction of the "true" β -ray angular distribution parameters from the observed angular distributions (i.e., correcting for background effects and determining analyzing efficiencies and experimental geometries). These difficulties are reflected in the nonstatistical scatter of the results of measurements of the parameter

y determined at various laboratories using either of the two techniques.

The circular polarization technique suffers particularly from the low efficiencies associated with coincidence counting and circular polarization analysis. A significant drawback of the nuclear orientation technique is the electron scattering from the metallic apparatus, necessary to achieve ultralow temperature nuclear orientation, in the vicinity of the sample. At best one hopes that the two methods will serve somewhat to complement each other, and a complete determination of the parameters of allowed decays should represent results from both methods. Unfortunately, the experimental activity in this area, particularly as regards application of the nuclear orientation technique, was largely confined to a few years immediately subsequent to the discovery of parity violation in weak interactions (by means of the first successful experimental study of β emission from polarized nuclei.⁶) In the intervening years, advances in particle detectors, low-temperature technology, and nuclear polarization techniques have provided an impetus for reapplying the nuclear orientation technique to this problem. The present report describes determinations of the positron β -ray asymmetry in the decay of oriented ⁵²Mn employing two independent and somewhat novel detection methods: (1) use of a long-focusing solenoid to guide the positrons to an intrinsic Ge detector, and (2) the coincident detection of the two positron annihilation photons. The first method was used in a series of experiments that were completed in 1972. The resulting value of $y = C_{\nu}M_{\nu}/C_{\nu}M_{\text{GT}}$ was much larger in magnitude than any of the published values. Although we were very confident that this result was correct, especially because a large asymmetry was present even in the raw data, we nevertheless felt it prudent to delay publication until an independent confirmation could be made. Consequently the apparatus was rebuilt and another experiment was carried out using the second method.

The theory of this type of measurement is recapitulated briefly in Sec. II. Experiments are described in more detail in Sec. III. Sec. IV describes data analysis. The results are given in Sec. V and discussed in Sec. VI.

II. THEORY

The theory of allowed β emission from polarized nuclei has been described in numerous reviews; for example, that of Schopper.¹ Radiation emitted from an oriented nucleus is in general described by

$$W(\theta) = \sum_k Q_k B_k U_k A_k P_k(\cos\theta), \quad (1)$$

where the Q_k are the solid angle correction factors, B_k are orientation parameters describing the degree of orientation of the emitting nuclear state, U_k are deorientation parameters which correct for the effect of unobserved intermediate radiations, A_k are angular distribution coefficients which depend on the properties of the observed radiation, and P_k are Legendre polynomials evaluated at the angle θ between the emission direction and the polarization direction. In the case of allowed β emission, the angular distribution function becomes (assuming T invariance, maximal P violation, and no second forbidden contributions):

$$W_{\beta}(\theta) = 1 + Q_1 B_1 A_1(\beta) \cos\theta, \quad (2)$$

where (for a $\Delta I = 0$ transition)

$$A_1(\beta) = \frac{[b_1(01) + b_1(10)]F_1(01II) + b_1(11)F_1(11II)}{b_0(00) + b_0(11)}, \quad (3)$$

where the β -particle parameters are as given by Alder, Stech, and Winther,⁷ who also tabulate the F coefficients. Here some care must be exercised in accounting for the phases involved in the calculation, and in fact one obtains an error in the phase of the odd-order terms of the angular distribution when using the above angular distribution coefficients with the orientation parameters B_k of Blin-Stoyle and Grace.⁸ This point has been discussed in a recent tabulation of the orientation parameters.⁹ Although the convention adopted is irrelevant with respect to the final result, the choice of the phase used in the present work permits the odd-order angular distribution coefficients A_k to be written in a manner analogous to the case of γ radiation, in terms of particle parameters (which are simply the multipole matrix elements for γ rays) times F coefficients.

The angular distribution parameter reduces directly to

$$A_1(\beta) = \frac{2}{3} \frac{v}{c} \frac{yF_1(01II) + F_1(11II)}{1 + y^2}, \quad (4)$$

where $y = C_{\nu}M_{\nu}/C_{\nu}M_{\text{GT}}$.

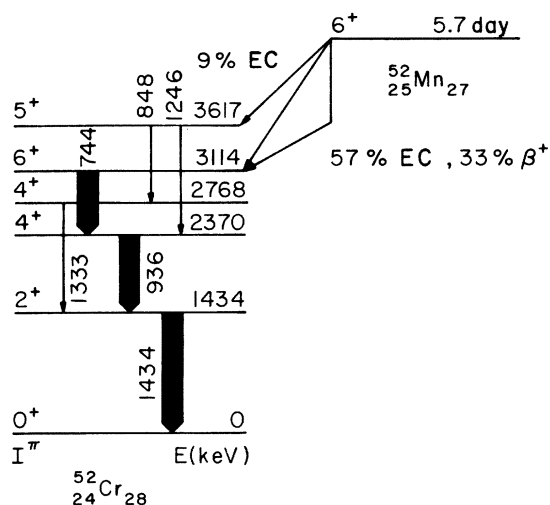
Since the experiment actually measures a continuous β spectrum, the dependence on the β -particle energy E must be included, and we consider then a correlation function $W_{\beta}(\theta, E)$ of the form

$$W_{\beta}(\theta, E) = N(E)[1 + Q_1 B_1 A_1(\beta) \cos\theta], \quad (5)$$

where $N(E)$ gives the probability of β emission between the energies E and $E + dE$.

$$N(E) = N_0 E(E^2 - 1)^{1/2} (E_0 - E)^2 F(Z, E), \quad (6)$$

with the energy E and end-point energy E_0 measured in units of $m_e c^2$. The β -particle kinetic energy is thus equal to $E - 1$, and the ratio v/c is given by $(E^2 - 1)^{1/2}/E$.

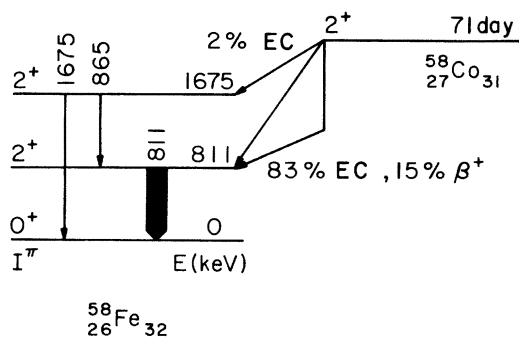
FIG. 1. Partial decay scheme of ^{52}Mn .

In the present work, the angular distribution of the allowed β emission from ^{52}Mn has been observed, and similar studies of the β emissions from ^{58}Co and ^{60}Co were done for calibration and checks on the apparatus. The relevant features of the decay schemes of these isotopes are shown in Figs. 1-3.¹⁰ In Table I we summarize for convenience some of the relevant parameters of the decays. The hyperfine splitting Δ (the energy difference between adjacent magnetic substates) is obtained as $\Delta = \mu H / I k_B$, where μ is the nuclear moment (in nuclear magnetons μ_N), H is the hyperfine magnetic field of the impurity in an iron host lattice, and k_B is the Boltzmann constant. For a pure Gamow-Teller decay $I_i \rightarrow I_f$, such as that of ^{60}Co ,

$$A_1(\beta) = \pm \frac{2}{3} \frac{v}{c} F_1(11I_f I_i), \quad (7)$$

where \pm indicates β^\pm .

The orientation parameters of the parent level

FIG. 2. Decay scheme of ^{58}Co .

may be determined from the γ -ray angular distribution using Eq. (1),

$$W_\gamma(\theta) = 1 + Q_2 B_2 U_2 A_2 P_2(\cos\theta) + Q_4 B_4 U_4 A_4 P_4(\cos\theta). \quad (8)$$

All of the isotopes studied emit pure $E2$ transitions which can be used for thermometry purposes.

III. EXPERIMENTAL

A. Low-temperature apparatus

The essential features of the low-temperature apparatus and the techniques of sample preparation were common to both the β -particle and annihilation-photon experiments. The sample mounting, radiation detectors, and electronics were different for the two experiments and will be described separately.

The samples were cooled to temperatures in the range of 8 mK, corresponding to a ^{52}Mn polarization of 75%, by means of the adiabatic demagnetization of cerium magnesium nitrate. The Dewar system employed to maintain the cryostat at temperatures of 1 K is shown in Fig. 4. This system was originally designed with the possibility of a time-reversal experiment in mind. Such an experiment requires a β - γ coincidence measurement, and the sensitivity is maximized when the angle between the direction of emission of β and γ is 45° . For this reason the tail section of the Dewars has been beveled at 45° to facilitate placement of the γ detectors.

The liquid nitrogen-liquid helium Dewar system and 50-kOe cooling magnet were of conventional design. Further details of the construction may be found in a more detailed account of the positron detection experiments.¹¹

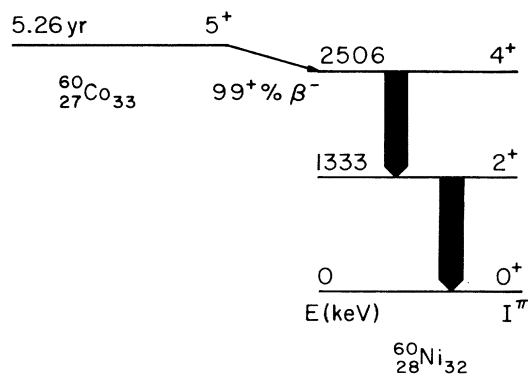
FIG. 3. Partial decay scheme of ^{60}Co .

TABLE I. Relevant decay properties of ^{52}Mn , ^{58}Co , ^{60}Co .

Parent nuclide	I_i	I_f	μ^a (μ_N)	H^b (kOe)	Δ (mk)	End-point energy (keV)		
							$F_1(01I_fI_i)$	$F_1(11I_fI_i)$
^{52}Mn	6	6	+3.062	-227.0	4.24	575	1.732	-0.134
^{58}Co	2	2	+4.044	-287.7	21.3	474	1.732	-0.354
^{60}Co	5	4	+3.799	-287.7	8.01	313	...	-0.949

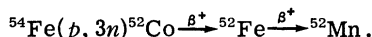
^a V. S. Shirley, in *Proceedings of the International Conference on Hyperfine Interactions Studied in Nuclear Reactions and Decay*, edited by E. Karlsson and R. Wappling (Uppsala, Upplands Grafiska AB, 1974).

^b T. Koster and D. A. Shirley, in *Hyperfine Interactions in Excited Nuclei*, edited by G. Goldring and R. Kalish (Gordon and Breach, New York, 1971), p. 1239.

B. Sample preparation

The ^{52}Mn activity was obtained by proton irradiation of natural iron foils. In this way the activity is produced *in situ* in a ferromagnetic environment, obviating the need for chemical separation and the other sample preparation techniques normally associated with nuclear orientation measurements. Foils of 10 mg/cm^2 ($12.7 \mu\text{m}$) thickness were employed; in the case of the positron measurement, the foils were rolled to 6 mg/cm^2 . These thicknesses provided a reasonable compromise between the desirability of thin foils for reducing scattering of the β particles and the corresponding reduced thermal conductivity of such thin foils, which may reduce the degree of nuclear polarization that can be attained.

The foils were irradiated with 32-MeV protons from the LBL 88-in. cyclotron. Currents of $5 \mu\text{A}$ were used, which were low enough to prevent burning of the foils. The activity was produced by means of the reaction



The ^{52}Co and ^{56}Co activities also produced did not interfere with the experiment; the 18-h ^{55}Co was allowed to decay away, and the ^{56}Co activity was considerably weaker than the ^{52}Mn .

The ^{60}Co and ^{58}Co samples were produced from activity obtained commercially in HCl solution. The activity was evaporated onto iron foils and reduced under H_2 . The foils were melted and then rolled to thicknesses in the range of 10 mg/cm^2 ($12.7 \mu\text{m}$).

All foils were annealed prior to being soldered to the cold finger of the apparatus using (non-superconducting) Bi-Cd solder.

C. Apparatus

1. Positron measurements

A schematic representation of the lower tail section of the cryostat is shown in Fig. 5. An intrinsic germanium detector of 0.8 mm thickness (0.5 mm depletion depth) was used for the posi-

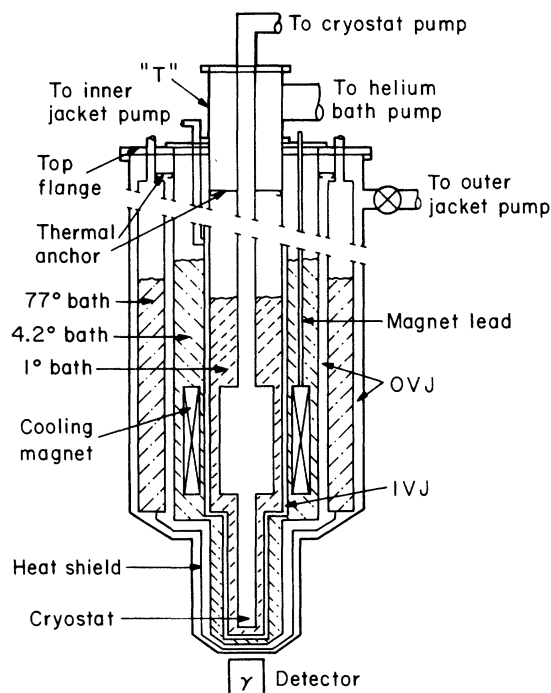


FIG. 4. A schematic diagram of the Dewar system. OVJ is Outer Vacuum Jacket, in which aluminized Mylar "superinsulation" was used to reduce radiation into the Dewars; IVJ is Inner Vacuum Jacket; 77 K bath is liquid nitrogen at atmospheric pressure; 4.2 K bath is liquid helium at atmospheric pressure; 1 K bath is liquid helium pumped to a pressure of $60 \mu\text{m}$.

trons. The area of the detector was 0.63 cm^2 , and with the 0.64-cm diam collimator, the solid angle subtended by the detector at the source was 0.03%.

The intrinsic Ge detector employed in the present work provided the advantage of the superior energy resolution normally associated with solid-state detectors, while not exhibiting the loss in performance which would have been characteristic of the more conventional lithium-drifted detectors when the detector housing was periodically warmed in order to change samples.

The principal difficulties associated with this type of experiment arise from either (a) the response of the detector to unwanted events, mainly γ rays and Compton-scattered electrons, or (b) positrons which are backscattered from the detector, resulting in incomplete energy deposition. The γ response of the detector is minimized by using as thin a detector as possible. The Compton electrons are a potentially more serious problem; for every positron emitted in the ^{52}Mn decay, there are about nine high-energy γ rays emitted. These

γ rays can be Compton-scattered from the sample, the chamber walls, and the copper cold finger. The use of a long-focusing solenoid (which also provides the external polarizing field for the sample) serves to optimize the β -particle detection efficiency relative to that of the Compton electrons. The magnetic field of the solenoid guides the β particles from the source to the detector, while electrons which originate elsewhere spiral along the field lines and tend to be absorbed eventually by the cryostat walls or the detector collimator. The geometry was arranged such that the detector and source were each placed 2.5 cm in from the opposite ends of the solenoid. The solenoid was operated at a field of 10.5 kOe.

The detector chamber provided a vacuum independent of the cryostat, a thin Mylar entrance window for the positrons, and a detector mounting thermally anchored at 1 K. The performance of germanium detectors is at best unpredictable at temperatures below 10 K; optimum performance is generally obtained when the detector is warmed (as, for example, with a resistance heater) to temperatures of $\sim 20 \text{ K}$. The intrinsic germanium detector employed in the present work operated well down to 1 K, but had a tendency to polarize (due to trapped charges) after a period of 12 h. It was found that the application of a forward bias voltage of 1–2 V was sufficient to sweep out the trapped charges.

The electronic system consisted of conventional linear pulse amplifiers and discriminators. The digitized positron energy spectra were written onto magnetic tape for subsequent computer analysis.

2. Annihilation photon measurements

A schematic diagram of the lower tail section of the cryostat employed in the annihilation photon measurement is shown in Fig. 6. Positrons emitted by the source were stopped in the 2-mm thick bottom cap of the cryostat tail section (a relatively smaller number which are stopped in the lower section of the cryostat wall may be taken into account in the calculation of the geometrical correction factors). The annihilation gives rise to two 511-keV photons emitted in opposite directions. These are collimated somewhat by means of the lead collimator shown in Fig. 6; a sufficient amount of lead was used to prevent radiations from the sample from reaching the detectors directly. The two photons were further collimated by detecting the pair in coincidence using a pair of 7.6-cm by 7.6-cm NaI(Tl) detectors. (In actuality two independent pairs of detectors were used to increase the rate of data accumulation; these pairs were oriented at right angles to one another.) The effectiveness of the shielding

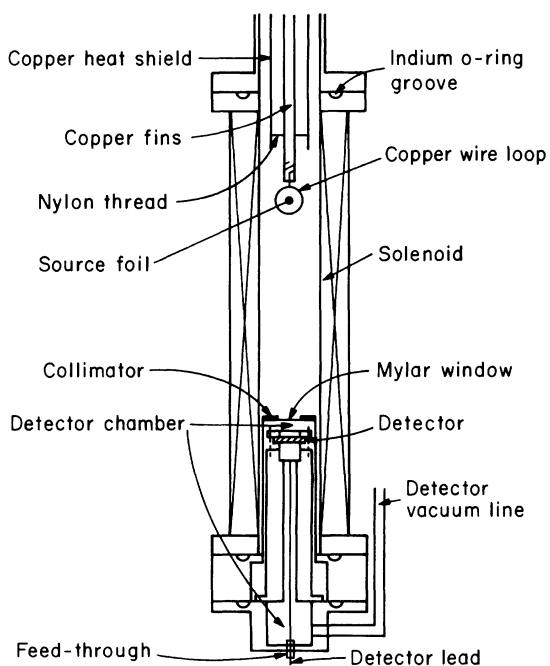


FIG. 5. Cryostat tail section used for direct measurement of positron asymmetry. The paramagnetic salt (CMN) is in contact with a series of copper metal fins, which eventually become the cold finger to which the sample is attached. The sample itself is soldered to a copper wire loop which is in turn attached to the cold finger. The intrinsic Ge detector is housed in its own vacuum chamber. The solenoid (2.5 cm diameter by 14 cm length) provides a magnetic field parallel to the axis of the cryostat; this field serves to polarize the sample as well as to focus the positrons toward the detector.

and collimation were tested by raising and lowering the sample relative to the detector and shielding assembly. The only change in the observed coincidence rate was that due to the change in solid angle subtended at the source by the end cap. Furthermore, the entire detector and shielding assembly could be raised or lowered by about 1 cm with no change in the count rate. The coincidence spectrum revealed only the presence of the 511-keV γ ray, and thus the energy interval accepted by the single-channel analyzer could be set quite wide with no fear of accepting spurious counts. Such widths are necessary to eliminate the possibility that changes in the applied polarizing field would affect the detector photomultiplier tubes and produce a gain shift in the energy analysis. Widths of the order of ± 200 keV were used, and no changes in count rate were observed with fields up to 3 kOe.

This arrangement eliminates a number of the difficulties associated with the direct measurement of the positrons, in particular (1) backscattering, since only those positrons which stop completely in the "detector" are counted, and (2) sensitivity of the solid-state detector to Compton electrons and photons, since this system has no sensitivity to either. However, these advantages are offset by a loss of the positron energy resolution—all positrons are counted, regardless of energy, and the observed counting rate represents

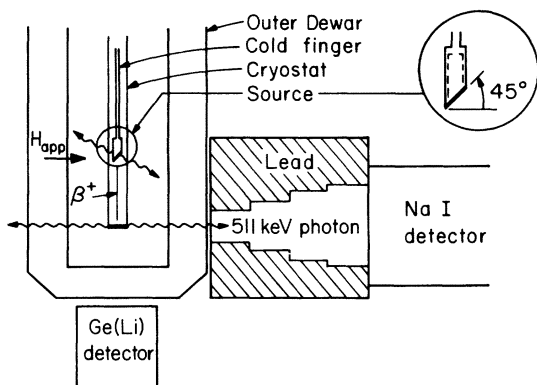


FIG. 6. Cryostat tail section, detector, and shielding used for indirect measurement of positron asymmetry by annihilation radiation. Positrons stopping in the bottom of the cryostat create two 511-keV photons emitted in opposite directions. These are detected in coincidence (second detector not shown). Lead shielding prevents radiation from the source itself from reaching the detector. For annihilation which takes place within the source, one of the photons may have a small probability of reaching one of the counters, as shown; however, the other photon would have zero probability of being counted, and hence this coincidence requirement serves to strengthen the collimation conditions.

an average of the angular distribution over the positron energy range. Although this would appear to be a serious effect, the angular distribution function depends not directly on the positron energy but rather on v/c , which varies relatively slowly over the energy spectrum. Furthermore, the effects of scattering within the source foil and of the magnetic field on the curvature of the positron paths serve to reduce the number of low-energy positrons which reach the scatterer; it is in the low-energy region that v/c varies most rapidly with positron energy.

The samples were prepared as described in Sec. III B and were soldered to an extension of the cold finger which was oriented at an angle of 45° relative to the scatterer. Backscattering in the vicinity of the source was reduced somewhat by hollowing out the inside of the source holder. The samples were polarized by means of two mutually perpendicular Helmholtz pairs, aligned so that one pair produced the field shown as H_{app} in Fig. 6, while the other could produce a field normal to the plane of the figure. The latter situation was used to provide a measure of $W_\gamma(90^\circ)$ for the determination of the degree of alignment of the nuclei, while the former field is that used for the positron measurements, and provided a nuclear polarization direction (in the plane of the foil) at 135° or 45° relative to the direction of detection. In this geometry of sample and coils, the positrons were emitted normal to the external polarizing field, and were thus subject to considerable Lorentz forces. For this reason the magnitude of the polarizing field was kept as small as possible. It was found that no significant loss of polarization was obtained in fields down to 0.6 kOe, if the sample was first saturated in a field of 2 kOe; however, applied fields greater than 1 kOe resulted in substantial ($> 50\%$) losses in count rate, owing to the bending of the paths of the positrons such that they collided with the cryostat walls before reaching the bottom of the cryostat.

IV. PROCEDURE AND DATA ANALYSIS

A. β^+ measurements

Following demagnetization, the sample was polarized in an external field of 10.5 kOe directed away from the β detector. Six 10-min runs were taken; after each run the detector was slightly forward-biased in order to sweep out the trapped charges and avoid polarization of the detector. The polarizing field was then reversed for an additional six 10-min runs. Finally, the salt pill was warmed up to 1 K and three runs were taken with the field in each direction.

During the data accumulation, the sample tem-

perature was monitored by observing the anisotropy of the 744-keV γ ray with a Ge(Li) detector. During the experiment the temperature remained constant at 8 mK, corresponding to a polarization of 76%.

The theoretical β anisotropy was given previously as

$$W_{\beta}(\theta = 0^{\circ}) = 1 + \frac{v}{c} Q_1 \bar{A}_1 B_1, \quad (9)$$

where we have factored out the v/c dependence [$A_1 = (v/c)\bar{A}_1$]. In order to extract the β angular distribution from the observed spectra, a number of corrections were necessary. These are discussed below; the general effect of these corrections is to compensate for a difference between the "true" v/c and the "observed" v/c .

1. Compton electrons

If the detector is sensitive to Compton electrons from scattered γ rays (or to the γ rays themselves), an additional term is introduced into the angular distribution of the form $f_c W_{\gamma}$, where f_c is the fraction of events which arise from this source (estimated to be of the order of 10%) and W_{γ} is the γ -ray angular distribution, which we take to be represented by $W_{\gamma}(\theta = 0^{\circ})$. Thus the observed angular distribution W is given by

$$W = W_{\beta} + f_c W_{\gamma}, \quad (10)$$

and if we consider the difference in counting rates between the two field directions $\theta = 0^{\circ}$ and $\theta = 180^{\circ}$, we obtain

$$\frac{W(0^{\circ}) - W(180^{\circ})}{2\bar{W}} = \frac{\beta Q_1 \bar{A}_1 B_1}{1 + f_c}. \quad (11)$$

Here the warm isotropic counting rate is given by $\bar{W} = 1 + f_c$ ($W_{\beta} = W_{\gamma} = 1$ at high temperatures), and we have written $\beta = v/c$. Similarly,

$$\frac{W(0^{\circ}) + W(180^{\circ})}{2\bar{W}} = \frac{1 + f_c W_{\gamma}}{1 + f_c}. \quad (12)$$

$$W = W_{\beta} + f_c W_{\gamma} + W_{\beta e} + W_{\beta \gamma} + W_s \quad (16a)$$

$$= \frac{1 + \beta \alpha_1 + f_c W_{\gamma} + f_{\beta e} W_{\gamma} (1 + \beta' \alpha_1) + f_{\beta \gamma} (1 + \beta'' \alpha_1) + f_s (1 + \beta''' \alpha_1)}{1 + f} \quad (16b)$$

$$= 1 + \langle \beta \rangle \alpha_1 + \frac{(W_{\gamma} - 1)(f_c + f_{\beta e})}{1 + f}, \quad (16c)$$

with $f = f_c + f_{\beta e} + f_{\beta \gamma} + f_s$, and $\alpha_1 = Q_1 B_1 \bar{A}_1$, and where the average β is given by

$$\langle \beta \rangle = \beta \frac{1 + (\beta'/\beta) W_{\gamma} f_{\beta e} + (\beta''/\beta) f_{\beta \gamma} + (\beta'''/\beta) f_s}{1 + f}. \quad (17)$$

If W_{γ} is taken as the 0° γ -ray counting rate, then f_c may be determined and the appropriate correction applied to Eq. (11).

2. Pileup

Pileup can occur between Compton electrons and positrons (estimated to contribute about 1% of the observed intensity) or between annihilation photons and positrons (5%). The effect of this pileup is to increase the counting rate in the high-energy region of the spectrum. The relative importance of the annihilation photons in giving rise to this effect was evidenced in the failure to observe any similar effect of comparable magnitude in the ^{60}Co spectra which were used for calibration purposes. The effect of these pileup contributions on the angular distribution is to introduce, into the energy region corresponding to β , a term corresponding to some lower β' . The contributions of the positron-Compton and positron-annihilation photon pileup terms may then be written, respectively, as

$$W_{\beta e} = f_{\beta e} (1 + \beta' Q_1 B_1 \bar{A}_1) W, \quad (13)$$

$$W_{\beta \gamma} = f_{\beta \gamma} (1 + \beta'' Q_1 B_1 \bar{A}_1), \quad (14)$$

where $f_{\beta e}$ and $f_{\beta \gamma}$ are the magnitudes of these pileup contributions.

3. Backscattering

The effect of those positrons which scatter out of the detectors without full energy deposition is to introduce, in the energy region corresponding to β , a contribution to the angular distribution corresponding to some larger β''' , which we write as

$$W_s = f_s (1 + \beta''' Q_1 B_1 \bar{A}_1). \quad (15)$$

The complete observed (renormalized) β angular distribution may then be written as

As before, we then obtain

$$\frac{W(0^{\circ}) - W(180^{\circ})}{2\bar{W}} = \frac{1 + \langle \beta \rangle \alpha_1}{1 + f} \quad (18)$$

and

$$\frac{W(0^\circ) + W(180^\circ)}{2\bar{W}} = \frac{1 + (W_\gamma - 1)(f_c + f_{\beta e})}{1 + f}. \quad (19)$$

Although it is impossible to separate the contributions from the various corrections, the over-all effect of the factor f may be estimated from Eq. (19), since $(W_\gamma - 1)$ is reasonably small (approximately -0.3). If one then assumes that the pileup and backscattering effects on $\langle\beta\rangle$ tend to cancel one another, the positron spectrum may be renormalized to facilitate extraction of the asymmetry parameter.

One additional correction which must be applied involves the calculation of the solid-angle correction factor Q_1 , which in general depends on the strength of the field and on the positron velocity, since the focusing effect of the long solenoid will be different for positrons having different velocities. The effective solid angle is of order π (25%) for the range of β energies considered in this work, with the half-angle of the detector ranging from 65° ($\beta=0.6$) to 52° ($\beta=0.88$). The computed values of the solid-angle correction factor varied between 0.7 and 0.8 for the experimental geometry.

B. Annihilation photon measurements

Following demagnetization, the sample was polarized in an external field of 2 kOe oriented at 90° relative to the direction of the γ -ray detector (and also of the positron absorber). The γ -ray anisotropy in this configuration was used to deduce the polarization of the sample. The current in that pair of coils was then reduced to zero and the current in the other pair turned up such that the 45° field (relative to the positron absorber) was 2 kOe. This field was sufficient to saturate the internal field of the iron foil; however, it was also sufficiently large to prevent a larger number of positrons from reaching the absorber due to deflection by the field. The field was then reduced to 0.6 kOe; this magnitude was determined empirically as a fair compromise between the necessity of maintaining a reasonable degree of polarization in the sample and the desirability of having the smallest possible curvature of the path of the positron.

Even at these low applied fields, this curvature was considerable. In general the result of such curvature is to prevent low-velocity positrons from reaching the bottom absorber, since they now are bent into paths of large curvature and collide with the walls. The entire problem is somewhat more complex, however, since one must not only consider the effect on the polar angle θ (nominally 45°) but also on the azimuthal angle ϕ . We have computed the positron paths numerically from the theoretical expressions for

the off-axis fields of a Helmholtz pair; the result of this computation gives us a relationship between the polar angle θ and positron energy, and also a lower cutoff energy E_{\min} , below which the geometry of our experiment would prevent the annihilation photons from being counted.

Assuming the polar angle can be represented by a deviation angle α relative to 45° or 135° (depending on the direction of the hyperfine field), we compute the asymmetry

$$\alpha = \frac{W(\uparrow) - W(\downarrow)}{W(\uparrow) + W(\downarrow)}, \quad (20)$$

where the arrows indicate symbolically the applied field direction. For the geometry of the present experiment

$$\alpha = \frac{W(45^\circ - \alpha) - W(135^\circ + \alpha)}{W(45^\circ - \alpha) + W(135^\circ + \alpha)}, \quad (21)$$

using Eq. (5) for the β angular distribution and averaging over the β energies (due to the lack of energy resolution), we obtain

$$\alpha = \frac{\int N(E)dEQ_1 B_1 A_1 \cos 45^\circ (\sin \alpha + \cos \alpha)}{\int N(E)dE} \quad (22a)$$

$$= \frac{B_1 \bar{A}_1 \cos 45^\circ \int N(E)dE(v/c)Q_1 (\sin \alpha + \cos \alpha)}{\int N(E)dE}. \quad (22b)$$

We have taken $\alpha = \alpha(E)$, and have written $A_1 = \bar{A}_1 v/c$. The integrals are carried out from some cutoff energy E_{\min} to the β end-point energy E_{\max} . The energy E_{\min} is determined by the orbital considerations discussed above, with a small additional correction applied to account for absorption within the source. In evaluating the solid-angle correction Q_1 we assume our absorber to be a black disk.

V. RESULTS

A. Positron measurement

The result of the ^{60}Co measurement, following application of corrections (amounting to no more than 5% of the asymmetry) as described in Sec. IV A, was

$$\bar{A}_1 = 0.615 \pm 0.021,$$

which compares well with the expected value

$$\bar{A}_1 = -\frac{2}{3}F_1(1145) = 0.633.$$

The above experimental value represents a least-squares fit over the β energy range 140 to 280 keV, and the quoted uncertainty is three times the standard deviation of the least-squares fit. Figure 7 shows the raw and the corrected data. The good agreement between theory and experiment in the

case of ^{60}Co lends confidence to the ^{52}Mn results.

The raw and the corrected data for ^{52}Mn are shown in Fig. 8. A similar least-squares fit of the corrected (again $<5\%$) asymmetries between 105 and 560 keV yielded

$$\bar{A}_1 = -0.250 \pm 0.007.$$

Again the uncertainty represents three times the standard deviation of the least-squares fit.

B. Annihilation photon measurement

The annihilation photon (β^+) counting rates were determined for the two opposite field directions and the asymmetry computed according to Eq. (20). The orientation parameter B_1 was determined from the γ -ray anisotropy measurement, and this in turn permitted the parameter B_1 to be computed. The asymmetries were corrected for the B_1 , and the average values obtained were

$$^{58}\text{Co} \quad \alpha/B_1 = 0.060 \pm 0.002,$$

$$^{52}\text{Mn} \quad \alpha/B_1 = 0.074 \pm 0.006.$$

These results were corrected as described above, with an additional small correction included in the case of ^{58}Co to account for an apparent small deviation ($\sim 5^\circ$) of the plane of the foil from 45° (as determined from the γ -ray anisotropy). The corrected angular distribution parameters are then

$$\bar{A}_1(^{58}\text{Co}) = -0.217 \pm 0.018,$$

$$\bar{A}_1(^{52}\text{Mn}) = -0.235 \pm 0.027.$$

The results for ^{58}Co are in substantial agreement with the previous results of Andrews *et al.*¹² ($\bar{A}_1 = -0.243 \pm 0.007$) and indicate that the various correction factors have been reasonably well accounted for. The present results indicate $y = +0.016 \pm 0.016$ for ^{58}Co , which is consistent with previous studies.¹²

VI. DISCUSSION

Assuming maximal parity violation, time-reversal invariance, and vanishing second forbidden contributions the present results indicate a Fermi/Gamow-Teller mixing ratio of

$$y = -0.144 \pm 0.006 \quad (\beta^+),$$

$$y = -0.131 \pm 0.024 \quad (\gamma\gamma),$$

where β^+ and $\gamma\gamma$ refer to the positron and annihilation photon measurements, respectively.

There have been numerous previous studies of the allowed β decay of ^{52}Mn , using both the positron asymmetry^{13,14} and circular polarization techniques.¹⁵⁻²¹ These results and the corresponding deduced values of y are summarized in Fig. 9. As can be seen, there is considerable nonstatistical scatter in the various results, with the present

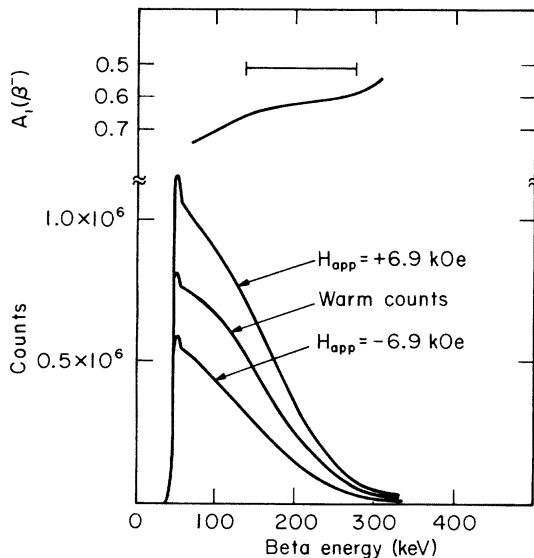


FIG. 7. Raw and corrected asymmetries from the decay of polarized ^{60}Co . The lower portion of the figure shows the actual spectra recorded for two orientations of the applied field and the isotropic warm counts. The upper portions shows the corrected asymmetries in terms of the β angular distribution parameter A_1 . The horizontal bar shows the energy region used in arriving at the final result.

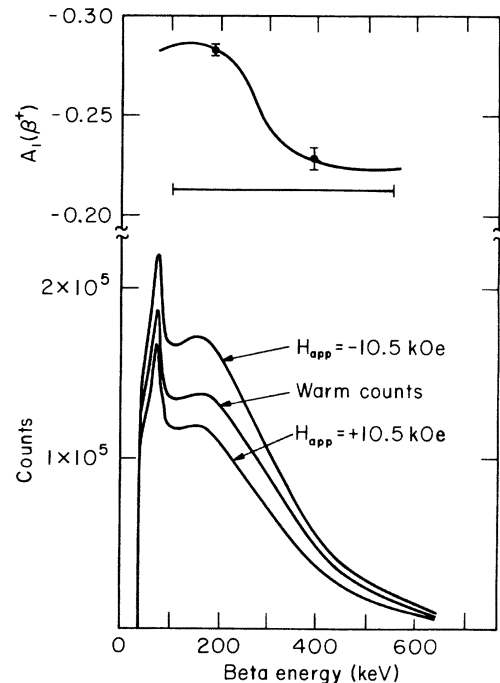


FIG. 8. Raw and corrected positron asymmetries from the decay of polarized ^{52}Mn . See caption to Fig. 7.

results showing evidence for the largest amount of Fermi/Gamow-Teller mixing yet attained.

The nuclear polarization results (Refs. 13, 14, and the present work) strongly favor nonvanishing negative values of y , while there seems to be no consistent trend among the results of the circular polarization correlations. These results are interpreted as

$$W_{\beta\gamma}(\theta) = 1 + (v/c)\tilde{B}_1(\beta)A_1(\gamma)\cos\theta, \quad (23)$$

where $\tilde{B}_1(\beta)$ is the angular orientation parameter describing the beta decay

$$\tilde{B}_1(\beta) = \frac{2}{3} \frac{-yF_1(01II) + F_1(11II)}{1 + y^2}, \quad (24)$$

in analogy with Eq. (4). Although several of the circular polarization results^{17,19,20} agree with the

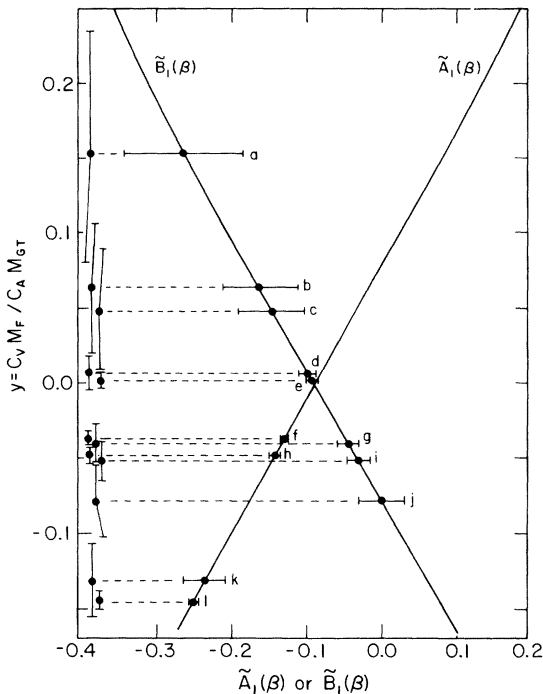


FIG. 9. Summary of results to date on the Fermi to Gamow-Teller mixing ratio y in the ^{52}Mn decay. The author's quoted results for the β angular distribution coefficient [$\tilde{A}_1(\beta)$, from experiments with polarized nuclei] and β angular orientation coefficient [$\tilde{B}_1(\beta)$, from circular polarization experiments] are shown on the theoretical curves of \tilde{A}_1 or \tilde{B}_1 vs y (these curves are linear for small y). The corresponding deduced values of y are shown on the left. References are: (a) Boehm (1958), Ref. 15; (b) Boehm (1962), quoted in Ref. 16; (c) Bloom *et al.* (1962), Ref. 16; (d) Mann *et al.* (1965), Ref. 18; (e) Pinogot (1971), Ref. 21; (f) Postma *et al.* (1958), Ref. 13; (g) Sawyer (1968), Ref. 20; (h) Ambler *et al.* (1958), Ref. 14; (i) Behrens (1967), Ref. 19; (j) Daniel *et al.* (1962), Ref. 17; (k) present work, $\gamma\gamma$; (l) present work, β^+ .

negative y values obtained in the polarized nuclei experiments, the most precise of the quoted circular polarization results^{18,21} indicate vanishing y values.

In comparing our result for ^{52}Mn with the earlier nuclear polarization measurements,^{13,14} we note that agreement may be obtained if account is taken of the differences in experimental conditions. Although the values of y deduced from the earlier work were lower than ours by a factor of 3, the observed values of A_1 were lower by only a factor of 1.6. Our experiments had the great advantage of being carried out in a ferromagnetic metal, in which high thermal conductivity ensured a uniform sample temperature. The hyperfine Hamiltonian was both simple and well known, and the warm-up rate was very low. The earlier nuclear polarization studies were done in the paramagnetic salt CMN—the only lattice then available. There are two inequivalent sites for the divalent ions in this material with different and rather complicated hyperfine Hamiltonians. The poor thermal conductivity and rapid heat-leak rates, which would cause the outer layers of the CMN crystals (from which the positrons that reached the counters were emitted) to be warmer than the rest, would reduce the apparent positron asymmetry below its true value. In the hundreds of nuclear orientation experiments that have been carried out in our laboratory using both paramagnetic salts and ferromagnetic metals as hosts, we have observed just this kind of discrepancy many times.²² An attenuation factor of ~ 1.6 is about what we would have expected from the paramagnetic salt work, under the circumstances of the early experiments.

The variations in the circular polarization results are more difficult to reconcile. The presence of impurity activities is unlikely to contribute to the differences, since the $^{52}\text{Cr}(p,n)^{52}\text{Mn}$ reaction used in the circular polarization studies produces no long-lived positron-emitting activities other than ^{52}Mn . Although there are variations in the β - and γ -ray discriminator levels used in the circular polarization work, there seems to be no direct correlation between the discriminator settings and the experimental asymmetry.

In comparing the nuclear polarization results with the circular polarization data several facts are inescapable:

- (1) The nuclear polarization method is very direct. A large asymmetry was obvious by visual inspection of the raw data. Any experimental problems tend to decrease the apparent asymmetry. The total range of all nuclear polarization results for ^{52}Mn (a factor of 1.6 in the observed asymmetry) is well understood.
- (2) The β - γ circular polarization correlation

method is not as direct, requiring a large correction factor to go from raw data to the asymmetry parameter A_1 . The measured A_1 values in the literature scatter badly.

(3) Finally, the nuclear polarization method is less susceptible in this case to any possible error in formulation of the theory. The magnitude of the observed asymmetry is much larger than would be expected from a pure Gamow-Teller transition: there must be a substantial Fermi admixture.

Although the present results do not shed additional light on the conflicting circular-polarization values in the literature for the Fermi/Gamow-Teller mixing ratio of the positron decay of ^{52}Mn , they do indicate the presence of a nonvanishing Fermi matrix element. The Fermi amplitudes would vanish for strict obedience to the isospin selection rules ($M_F = 0$ when $\Delta T \neq 0$; here $\Delta T = 1$), although it is perhaps doubtful that T can be regarded as a good quantum number for as heavy a nucleus as ^{52}Mn . The Fermi amplitude gives a measure of the degree of isospin impurity in the nuclear states, or, equivalently, of the size of the Coulomb matrix element which distorts the symmetry between protons and neutrons. While the scatter of the experimental results to date is large, the present results do provide evidence in support of a rather larger Fermi amplitude. In particular, based on the presently deduced value of γ , a Fermi matrix element $M_F = 0.017$ is deduced, with a corresponding isospin mixing amplitude of $\alpha = 0.009$ and a Coulomb matrix element $H_C = 70$ keV (these quantities are defined and discussed by Schopper¹).

Theoretical calculations of M_F are difficult owing to the uncertainty in the charge-dependent (i.e., isospin nonconserving) part of the nucleon-nuclear interaction. (A brief survey of the theory has been given by Blin-Stoyle.²³) Bouchiat²⁴ has calculated $M_F = 0.010$ considering the Coulomb potential only, and Kelly and Moszkowski²⁵ obtained $M_F = 0.006$ using a charge-dependent inter-nucleon potential. More recently Koyama, Takahashi, and Yamada²⁶ have computed values for M_F in the range 0.005–0.030 depending on the form of the energy distribution of final nucleon states. The present result is not inconsistent with any of these theoretical estimates. The magnitude of the presently measured value of γ suggests that ^{52}Mn would

be a reasonable candidate for a future study of time-reversal invariance in β decay.

APPENDIX

Because the notation used presently for the equations describing the β angular distribution $\beta(\theta)$ and β - γ circular polarization correlation $\beta\gamma_{\text{cp}}(\theta)$, differs from that in use at the time of most of the earlier work, we present below a brief comparison of the equations.

$\beta(\theta)$. In much of the early work, one finds this written as

$$W(\theta) = 1 + f_1(v/c)A\cos\theta. \quad (25)$$

Rewriting our Eq. (2), neglecting the factor Q_1 and factoring the v/c dependence as $A_1 = (v/c)\tilde{A}_1$,

$$W(\theta) = 1 + B_1(v/c)\tilde{A}_1(\beta)\cos\theta. \quad (26)$$

The orientation parameter B_1 is given in terms of the moment f_1 as⁹

$$B_1 = -\left(\frac{3I}{I+1}\right)^{1/2} f_1, \quad (27)$$

and the correspondence between A and \tilde{A}_1 then follows directly.

$\beta\gamma_{\text{cp}}(\theta)$. The earlier work generally uses the notation

$$W(\theta) = 1 + \tau(v/c)A\cos\theta, \quad (28)$$

where $\tau = \pm 1$ depending whether the circular polarization is right or left handed, and A includes factors depending on the β -decay properties as well as on the γ -ray parameters.¹⁸ In the present notation

$$W(\theta) = 1 + (v/c)\tilde{B}_1(\beta)A_1(\gamma)\cos\theta. \quad (29)$$

This notation shows explicitly the contributions of the β -decay γ ray to the quantity previously defined as A . The expression for $B_1(\beta)$ is as given in Eq. (24), and the γ -ray term is written in the usual way in terms of F coefficients.

The form of Eqs. (26) and (28) show a similarity to the equation used for general angular distribution and correlation experiments, and the identification of the various terms, while differing somewhat from that used in the various experimental papers cited, is derived directly from the original form given by Alder, Stech, and Winther.⁷

† Work performed under the auspices of the U. S. Energy Research and Development Administration.

* Present address: Student Affairs Office, School of Medicine, University of California, San Francisco,

California 94143.

‡ Present address: Department of Physics, Oregon State University, Corvallis, Oregon 97330.

¹H. F. Schopper, *Weak Interactions and Nuclear Beta*

- Decay* (North-Holland, Amsterdam, 1966).
- ²C. S. Wu and S. Moskowsky, *Beta Decay* (Wiley, New York, 1966).
- ³J. H. Christenson, J. W. Cronin, V. L. Fitch, and R. Turlay, *Phys. Rev. Lett.* **13**, 138 (1964).
- ⁴S. R. deGroot, H. A. Tolhoek, and W. J. Huiskamp, in *Alpha-, Beta-, and Gamma-Ray Spectroscopy*, edited by K. Siegbahn (North-Holland, Amsterdam, 1965), p. 1199.
- ⁵H. Frauenfelder and R. M. Steffen, in *Alpha-, Beta-, and Gamma-Ray Spectroscopy* (see Ref. 4), p. 997.
- ⁶C. S. Wu, E. Ambler, R. W. Hayward, D. D. Hoppes, and R. P. Hudson, *Phys. Rev.* **105**, 1413 (1957).
- ⁷K. Alder, B. Stech, and A. Winther, *Phys. Rev.* **107**, 728 (1957).
- ⁸R. J. Blin-Stoyle and M. A. Grace, in *Handbuch der Physik*, edited by S. Flügge (Springer-Verlag, Berlin, 1957), Vol. XLIII, p. 555.
- ⁹K. S. Krane, *Nucl. Data* **A11**, 407 (1973).
- ¹⁰C. M. Lederer, J. M. Hollander, and I. Perlman, *Table of Isotopes* (Wiley, New York, 1967).
- ¹¹S. T.-C. Hung, Ph.D. thesis, University of California Lawrence Berkeley Laboratory Report No. LBL-1256, 1972 (unpublished).
- ¹²H. R. Andrews, E. J. Cohen, T. F. Knott, and F. M. Pipkin, *Phys. Rev. C* **7**, 1851 (1973).
- ¹³H. Postma, W. J. Huiskamp, A. R. Miedema, M. J. Steenland, H. A. Tolhoek, and C. J. Gorter, *Physica* (The Hague) **24**, 157 (1958); see also result quoted by W. J. Huiskamp and H. A. Tolhoek, *Progress in Low Temperature Physics*, edited by C. J. Gorter (North-Holland, Amsterdam, 1961), Vol. III, p. 333. It should also be noted that the use of the annihilation photon technique in detecting positrons emitted by polarized nuclei was introduced by these investigators.
- ¹⁴E. Ambler, R. W. Hayward, D. D. Hoppes, and R. P. Hudson, *Phys. Rev.* **110**, 787 (1958).
- ¹⁵F. Boehn, *Phys. Rev.* **109**, 1018 (1958).
- ¹⁶S. D. Bloom, L. G. Mann, and J. A. Miskel, *Phys. Rev.* **125**, 2021 (1962).
- ¹⁷H. Daniel, O. Mehling, O. Müller, and K. S. Subudhi, *Phys. Rev.* **128**, 261 (1962).
- ¹⁸L. G. Mann, D. C. Camp, J. A. Miskel, and R. J. Nagle, *Phys. Rev.* **137**, B1 (1965).
- ¹⁹H. Behrens, *Z. Phys.* **201**, 153 (1967).
- ²⁰J. A. Sawyer, Ph.D. thesis, University of California Lawrence Livermore Laboratory Report No. UCRL-50440, 1968 (unpublished).
- ²¹O. Pingot, *Nucl. Phys.* **A174**, 627 (1971).
- ²²See, for example, M. Kaplan, J. Blok, and D. A. Shirley, *Phys. Rev.* **184**, 1177 (1969).
- ²³R. J. Blin-Stoyle, in *Isospin in Nuclear Physics*, edited by D. H. Wilkinson (North-Holland, Amsterdam, 1969), p. 117.
- ²⁴C. C. Bouchiat, *Phys. Rev.* **118**, 540 (1960).
- ²⁵P. S. Kelly and S. A. Moszkowski, *Z. Phys.* **158**, 304 (1960).
- ²⁶S. Koyama, K. Takahashi, and M. Yamada, *Prog. Theor. Phys.* **44**, 663 (1970).